

Supplementary Information

for

Magnetically Guided Chemical Locomotion of Self-Propelling Paperbots

Amit Kumar Singh,^a Tapas Kumar Mandal,^{*ab} and Dipankar Bandyopadhyay^{*ab}

^aCentre for Nanotechnology, ^bDepartment of Chemical Engineering,
Indian Institute of Technology Guwahati, Guwahati – 781039, India.

* Corresponding author: dipban@iitg.ernet.in, tapasche@iitg.ernet.in

Fabrication of magneto-catalytic paper microjets

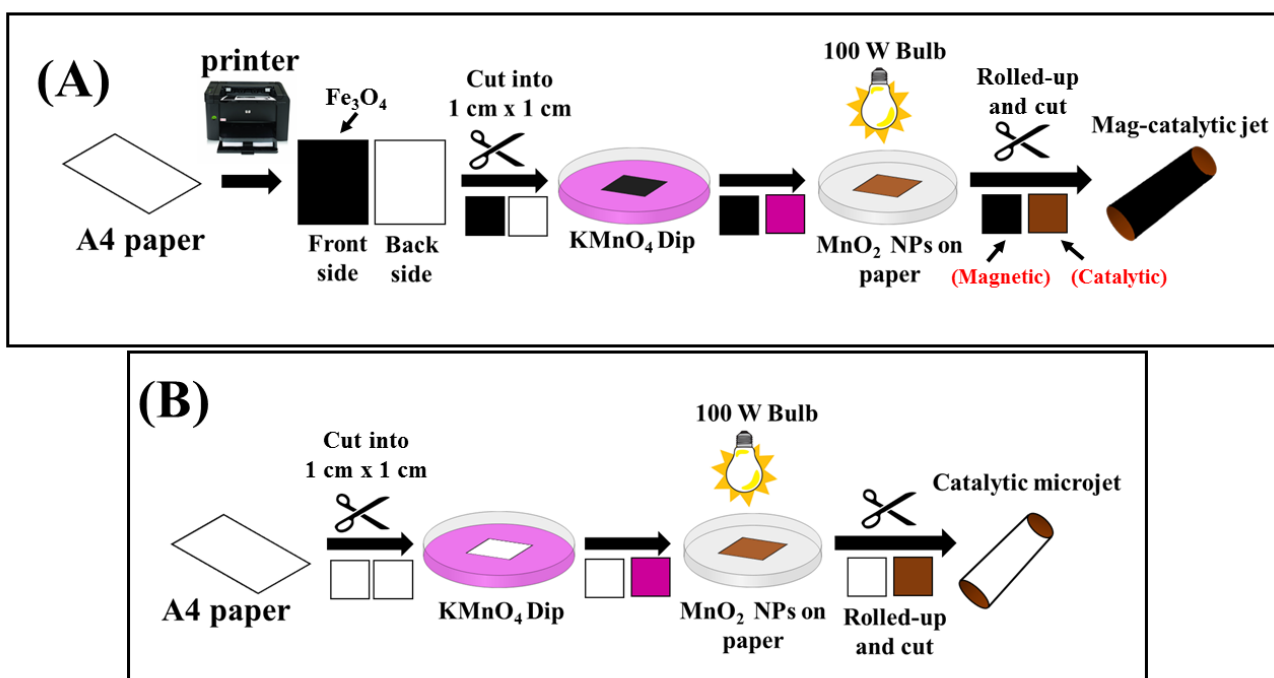


Figure S1. Fabrication of (A) magneto (Mag)-catalytic paper microjet and (B) catalytic paper microjet.

The microjet was fabricated using discarded paper sheets from the black and white laser jet printer (Figure S1 A). The one side of the flat piece of paper was uniformly coated with the toner ink of the

printer by taking a printout in black ink, which infused the magnetic sensitivity by depositing ferromagnetic layer of Fe₃O₄ microparticles on the paper surface.¹ Thereafter, the paper was cut into 1 cm × 1 cm square pieces. Following this, the manganese dioxide nanoparticles (MnO₂NPs) were deposited chemically on the non-printed side of the paper. The non-printed side of paper was dipped horizontally into a 0.45 M alkaline KMnO₄ (KMnO₄: NaOH = 1:1 in molar ratio) in such a way that the KMnO₄ makes a thin coating on the paper surface. Then the alkaline KMnO₄ coated paper was kept at room temperature for 10 h under a 100 W incandescent light exposure. The color of the paper surface changed from purple to brown due to formation of MnO₂NPs. The product was then washed with water and dried at 60 °C for 2 h. The detailed mechanism for formation of MnO₂NPs over cellulose fibers of paper have been previously explained by Wang *et al.*² The MnO₂NPs infused the chemical activation of the paper as the MnO₂NPs could catalytically decompose H₂O₂ ($2\text{H}_2\text{O}_2 \rightarrow 2\text{H}_2\text{O} + \text{O}_2$)³ when the paper was immersed inside a bath of peroxide fuel. After the deposition of MnO₂NPs, the flat piece of paper was rolled up manually and sealed with adhesive to form a tubular microjet where the toner ink coating stayed outside and the MnO₂NPs stays at the inner hollow core in the range of 300-600 μm. Thereafter, the tubular microjet was cut into pieces with a sharp surgical scissor of varying length ranging from 900 μm to 2 mm. The microjets of size ~ 900 μm with diameter opening of ~350 μm were used for all the experiments. The microjets were cut randomly and only those were selected for the experiments, which had significant difference in the diameter at the sides. This ensured that the shape of the microjet was similar to the frustum of a cylinder, which was verified through the microscopic inspections. For fabrication of catalytic microjet without the magnetic handle, a non-printed paper of dimension 1 cm × 1 cm was cut before following the steps mentioned previously to coat the MnO₂NPs, as shown in the Figure **S1 B**.

Fabrication of fluorescent catalytic paper microjets

The fluorescein sodium salt was dissolved in water to obtain 0.1 M solution. The solution was drop casted on the paper microjets and then the catalytic microtubes were dried at 40 °C for 2 h. The

fluorophore solution stained the cellulose fibers of the paper microjets making it fluorescent.⁴ The fluorescence activity is observed at UV excitation of 494 nm. The paper microjet appeared to be green in color (Figure S2 B).

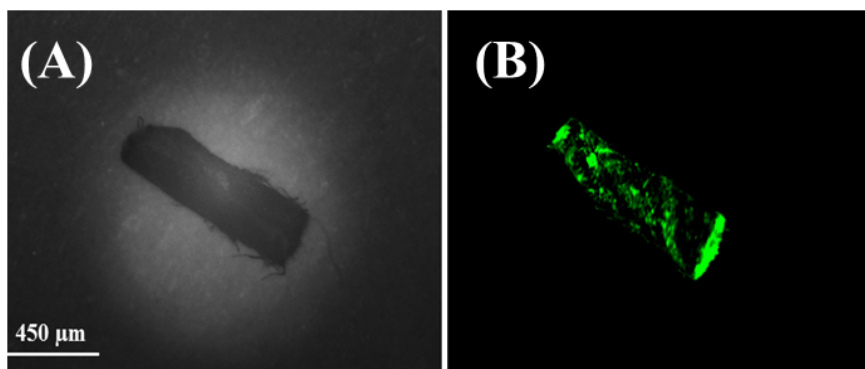


Figure S2. (A) The optical micrograph of tubular catalytic paper microjet ($\sim 900 \mu\text{m}$) at 2.5X magnification. (B) The fluorescein-tagged microjet observed under microscope at 494 nm excitation wavelength.

Rate constant measurement for H_2O_2 decomposition

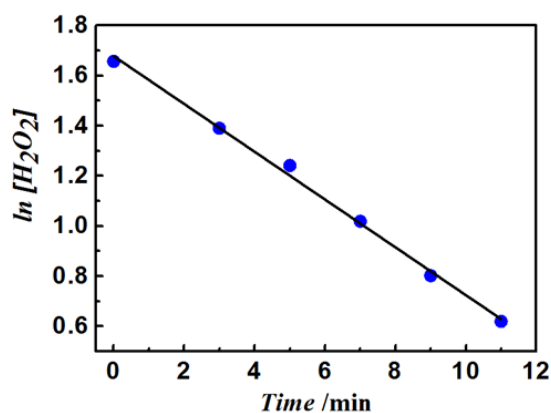


Figure S3. Rate constant (k) of 10% (v/v) H_2O_2 decomposition for one catalytic paper microjet.

Figure S3 shows the reaction kinetics for the 10% (v/v) hydrogen peroxide (H_2O_2) decomposition by a catalytic paper microjet. In presence of a catalytic microjet, the rate of decomposition of 10% (v/v) H_2O_2 followed first-order kinetics⁵ with the rate constant, $k = 0.095 \text{ min}^{-1}$.

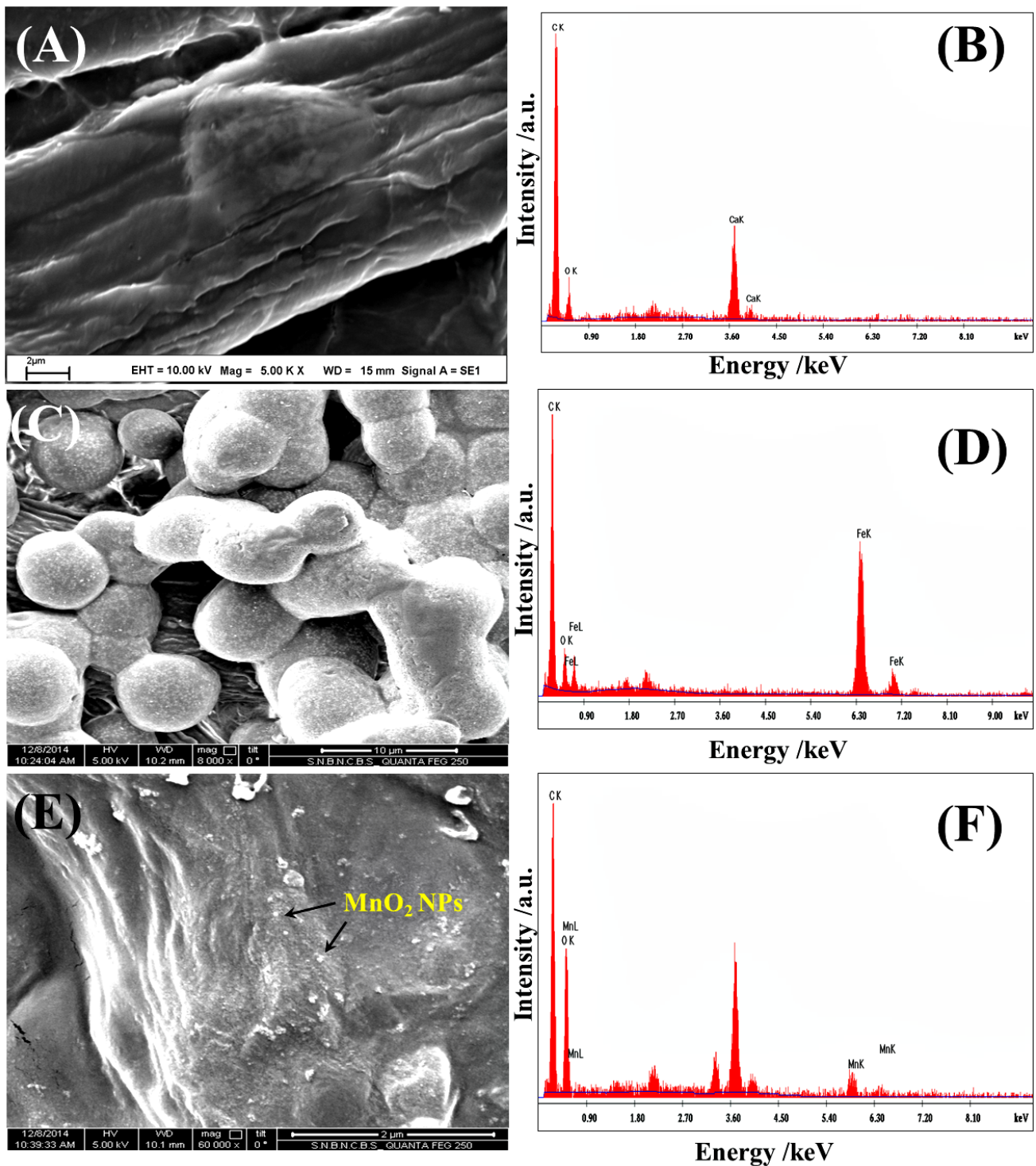


Figure S4. (A) Field emission scanning electron microscopy (FESEM) image of an uncoated cellulose fiber of printer paper. The scale bar at the bottom is of 2 μm . (B) Energy Dispersive X-ray (EDX) of the uncoated cellulose fiber. (C) FESEM image of a cellulose fiber of printer paper in which the Fe_3O_4 -microparticles were observed, which was distributed over the fiber surface. The scale bar at the bottom is of 10 μm . (D) EDX of Fe_3O_4 -based micro-globules on cellulose fibers shows the Fe and O peak. (E) FESEM image of a cellulose fiber coated with MnO_2 NPs. MnO_2 NPs were randomly distributed over the fibers surface. The scale bar at the bottom is of 2 μm . (F) EDX of a cellulose fiber coated with MnO_2 NPs shows the Mn and O peak.

The uncoated printer paper was characterized using Zeiss Sigma FESEM, operating at a maximum voltage of 10 kV and at magnification of 5.0 kx. FESEM image shows a single cellulose fiber of printer paper of width $\sim 13 \mu\text{m}$ (**Figure S4 A**). EDX of the uncoated cellulose fiber shows the carbon (C) and calcium (Ca) peaks (**Figure S4 B**). **Figure S4 C** and **E** were characterized using Quanta FEG250 FESEM, operating at a maximum voltage of 5 kV and at magnification of 8.0 kx and 60.0 kx, respectively. **Figure S4 C** shows the coalesced Fe_3O_4 -based microparticles of average radius $\sim 7 \mu\text{m}$. Thus, the figure confirmed that the magnetic toner ink of the printer deposited Fe_3O_4 microparticles while printing was performed. EDX of Fe_3O_4 -based microparticles on the cellulose fibers shows the presence of elemental iron (Fe), carbon (C), and oxygen (O) peaks (**Figure S4 D**). **Figure S4 E** shows the presence of the MnO_2 NPs on the cellulose fibres.⁶ The size of the MnO_2 NPs varied from 70 nm to 400 nm on the fibre surface. The EDX confirmed the presence of the MnO_2 NPs by showing the Mn and O peaks along with C and Ca peaks of the cellulose fibers. (**Figure S4 F**).

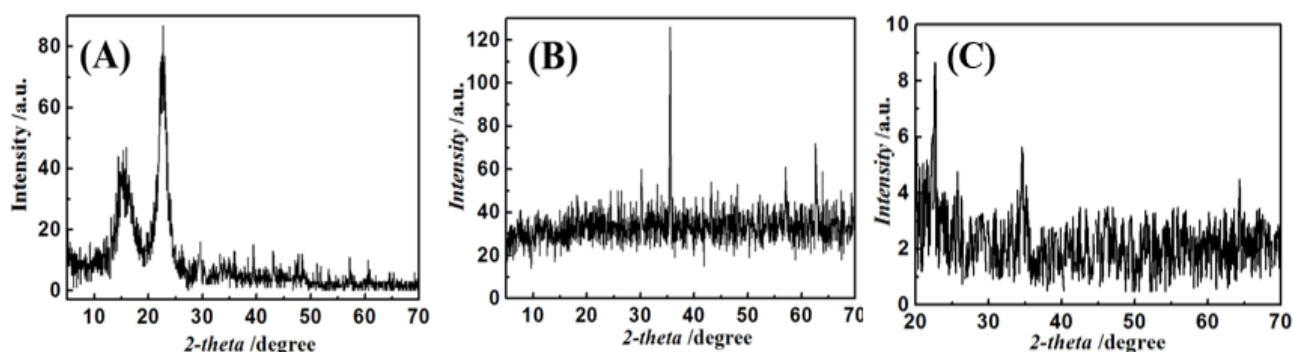


Figure S5. X-ray diffraction (XRD) of (A) uncoated printer paper, (B) toner ink and (C) MnO_2 NP-coated paper.

Figure S5 A shows XRD plot for non-printed paper. The plot displayed XRD patterns of microcrystalline cellulose-I with a primary peak at $2\theta = 22.7^\circ$, which corresponds to the (200) diffraction plane.⁷ This confirmed the presence of cellulose in the paper. The XRD of the toner ink (**Figure S5 B**) showed characteristic diffraction peaks at $2\theta = 30.1^\circ$, 35.5° , 43.15° , 62.6° corresponding to the (220), (311), (400), (440) crystallographic planes of magnetite (Fe_3O_4) particles

and thus confirmed the presence of magnetite in toner ink.⁸ **Figure S5 C** showed low intensity primary peak of cellulose at 22.6° and three weak peaks at $2\theta = 25.75^\circ$, 34.56° and 64.35° which corresponded to MnO_2NPs .^{6,9}

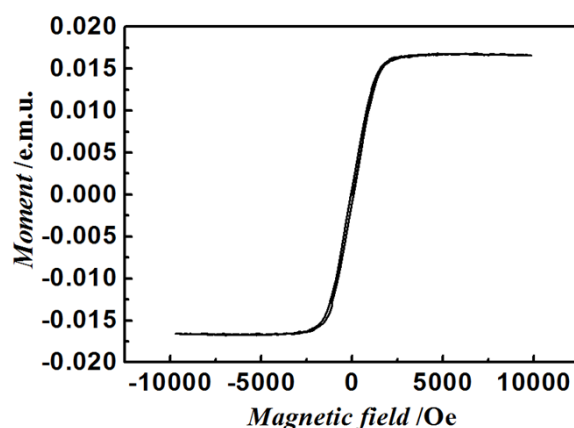


Figure S6. Vibrating sample magnetometry (VSM) hysteresis loop of a paper microjet with toner ink-coated outer wall.

Figure S6 was obtained from the VSM at 25°C by varying the magnetic field from -10 to 10 kOe. The magnetization curve suggested that the Fe_3O_4 coating on the outer surface of the paper microjet was soft ferromagnetic in nature and thus responsible for sensitivity of microjet towards applied magnetic field.

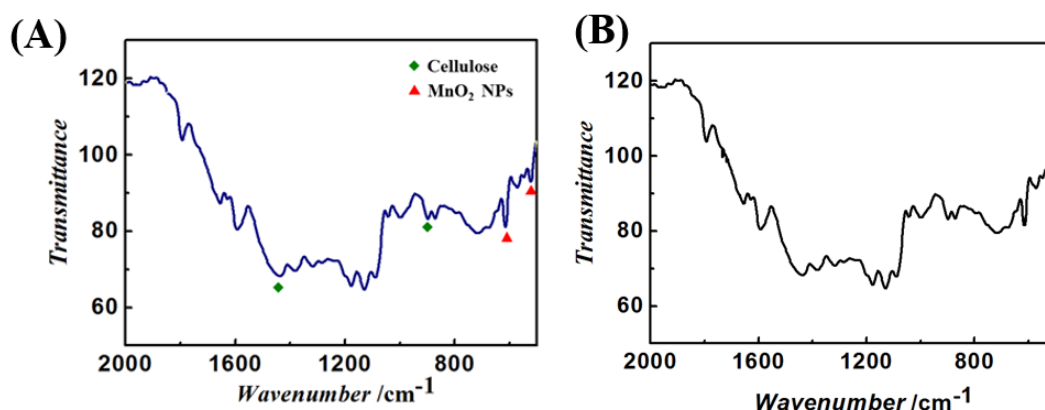


Figure S7. FTIR spectra of the MnO_2 NP-coated paper surface **(A)** before treatment and **(B)** after 5 min treatment with 9% H_2O_2 solution.

In the FTIR spectrum (**Figure S7**), the absorption band at 1427 cm^{-1} and 895 cm^{-1} could be assigned to a symmetric CH_2 bending vibration and C-O-C stretching at the β (1,4)- glycosidic linkage for the cellulose in the paper. The absorption bands at 519 cm^{-1} and 613 cm^{-1} corresponded to the stretching vibrations of the Mn-O and Mn-O-Mn bonds, respectively, confirming the presence of the MnO_2 NPs on the paper surface.⁶ The persistence of the characteristic peaks for MnO_2 in **Figure S7 B** suggests that catalytic MnO_2 NPs remained unaltered after peroxide treatment.

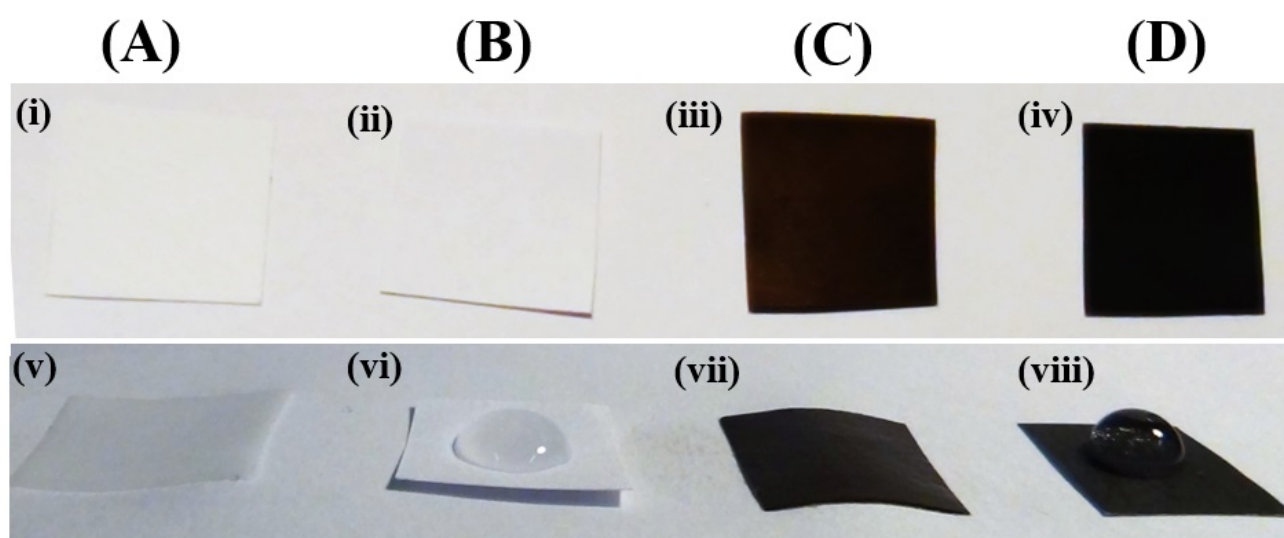


Figure S8. Photographs of (A) filter paper (B) uncoated printer paper (C) MnO_2 NP coated paper (D) printer toner ink coated paper.

Figure S8 shows the fate of a $100\text{ }\mu\text{L}$ of water droplet when dispensed (A) filter paper (B) uncoated printer paper (C) MnO_2 NP coated printer paper (D) printer toner ink coated paper. The color of the printer paper turned from white to dark brown⁶ after the deposition of MnO_2 NP on its surface (**Figure S8 C**) and white to black after taking the print from the printer (**Figure S8 D**). When dispensed, the water droplet got fully absorbed in the filter paper (**Figure S8 A (v)**) whereas showed partial wetting on the uncoated printer paper (**Figure S8 A (vi)**) and also on the paper coated with printer toner ink (**Figure S8 A (vii)**). The appearance of the droplet confirmed that the hydrophobicity of the paper coated with printer toner ink was larger than the non-coated one. In

comparison, the water droplet formed a thin film on the MnO₂NP coated printer paper (**Figure S8 A (viii)**). The experiment confirmed that, while the hydrophobicity of the outer printed side increased the lifetime of the microjet by increasing the time for dissolution, the wetting inner core ensured maximum contact of MnO₂NPs with the peroxide fuel for the chemical locomotion.

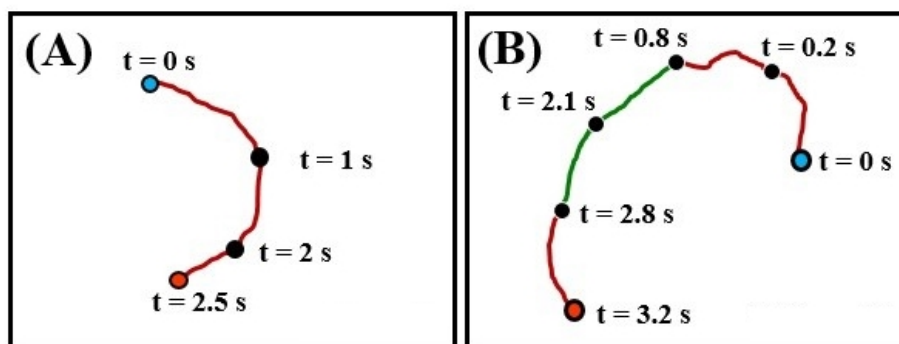


Figure S9. Motion trajectory of a (A) non-printed catalytic paper microjet in 16% (v/v) H₂O₂ solution (B) the coupled chemical and magnetophoretic locomotion of a catalytic paper microjet in 16% (v/v) H₂O₂ solution. The solid red lines shows the catalytic motion of the microjet and the green shows the motion in the presence of magnetic field. The blue circles and the red circles represent the initial and final position of the paperjet respectively.

Figure S9 A shows the motion trajectory of a non-printed catalytic paper microjet (~ 900 μm) inside a bath of 16% (v/v) hydrogen peroxide (H₂O₂) solution (as shown in **Video S1**) at various time intervals. **Figure S9 B** shows the motion trajectory for the coupled chemical and magnetophoretic locomotion of a ~ 900 μm catalytic paper microjet in 16% (v/v) H₂O₂ solution (as shown in **Video S4**).

SUPPORTING VIDEOS

Supporting Video S1: The video clip demonstrates the motion of a non-printed catalytic paper microjet (~ 900 μm) inside a bath of 16% (v/v) hydrogen peroxide (H₂O₂) solution. When the paper microjet was immersed in a 16% (v/v) aqueous peroxide solution, the O₂ bubbles were accumulated inside the tube due to the catalytic decomposition of the peroxide fuel on the MnO₂NPs at the inner hollow core. With progress in time, the bubbles grew and advanced towards one of the openings of

the microjet before ejected out of the microjet. The continuous ejection of the O₂ microbubbles from one side of the microtube provided the thrust for the motion.

Supporting Video S2: The video clip demonstrates a ~900 μm catalytic paper microjet in a bath of water (absence of H₂O₂). In this situation, no bubble ejection was observed from microjet and the microjet remained stationary during the course of observation. The experiment confirmed the microjet propulsion occurs only in presence of H₂O₂ as fuel.

Supporting Video S3: The video clip shows a ~900 μm paper microjet without inner MnO₂NPs coating suspended in a bath of 16% (v/v) H₂O₂ solution. In this situation, again the microjet remained stationary due to the absence of catalytic MnO₂NPs inside the inner hollow core. The experiment confirmed the propulsion by O₂ bubbles generated due to catalytic decomposition of H₂O₂ by MnO₂NPs.

Supporting Video S4: The video clip shows the coupled chemical and magnetophoretic locomotion of a ~ 900 μm catalytic paper microjet in 16% (v/v) H₂O₂ solution. While the catalytic MnO₂NPs inside the inner hollow core produced oxygen bubbles to produce the chemical locomotion, the external magnetic field induced a magnetophoretic motion to the microjet due to the presence of the magnetic Fe₃O₄ particles on the outer surface of the microjet. The video has been slowed down by 2x times.

Supporting Video S5: The video clip shows the motion of the catalytic microjet in aqueous 12% (v/v) H₂O₂ solution under microscope. The fluorescent tracer provided an optical indication of the local position of the paper microjet.

Supporting Video S6: The video clip shows the self-propulsion of the magneto-catalytic paperjet in 10% (v/v) peroxide solution (in the absence of magnetic field). The microjet shows catalytic propulsion in roughly straight-line trajectory.

Supporting Video S7: The video clip shows the steering of the self-propelling magneto-catalytic paperjet in 10% (v/v) peroxide solution with the help of a bar magnet.

Supporting Video S8: The video clip shows the magnetically-guided motion of a Rhodamine 6G-loaded paper microjet (~ 900 μm) inside a fuel-free water.

Supporting Video S9: The video clip shows the motion of a catalytic paper microjet (~ 900 μm) inside a bath of 10% (v/v) hydrogen peroxide (H_2O_2) solution. The speed of the microjet dropped with the decrease in the concentration of H_2O_2 fuel from 16% to 10%.

REFERENCES

- 1 M. Ataefard, *J. Compos. Mater.*, 2014, **0**, 1–9.
- 2 Y. Wang, X. Zhang, X. He, W. Zhang, X. Zhang and C. Lu, *Carbohydr. Polym.*, 2014, **110**, 302–308.
- 3 H. Wang, G. Zhao and M. Pumera, *J. Am. Chem. Soc.*, 2014, **136**, 2719–2722.
- 4 R. Pinto, A. L. Amaral, E. C. Ferreira, M. Mota, M. Vilanova, K. Ruel and M. Gama, *BMC Biotechnol.*, 2008, **8**, 1.
- 5 A. K. Singh, K. K. Dey, A. Chattopadhyay, T. K. Mandal and D. Bandyopadhyay, *Nanoscale*, 2014, **6**, 1398–1405.
- 6 L. Zhou, J. He, J. Zhang, Z. He, Y. Hu, C. Zhang and H. He, *J. Phys. Chem. C*, 2011, **115**, 16873–16878.
- 7 K. C. Cheng, J. M. Catchmark and A. Demirci, *J. Biol. Eng.*, 2009, **3**, 12.
- 8 M. Ma, Y. Zhang, Z. Guo and N. Gu, *Nanoscale Res. Lett.*, 2013, **8**, 16.
- 9 A. Shaabani, Z. Hezarkhani, S. Shaabani, *RSC Adv.*, 2014, **4**, 64419–64428.